

## **Acoustic Source Elevation Angle Estimates Using Two Microphones**

**by Kirsten A. Walker and W.C. Kirkpatrick Alberts, II**

**ARL-TR-6976**

**June 2014**

## **NOTICES**

### **Disclaimers**

The findings in this report are not to be construed as an official Department of the Army position unless so designated by other authorized documents.

Citation of manufacturer's or trade names does not constitute an official endorsement or approval of the use thereof.

Destroy this report when it is no longer needed. Do not return it to the originator.

# **Army Research Laboratory**

Adelphi, MD 20783-1197

---

---

**ARL-TR-6976**

**June 2014**

---

## **Acoustic Source Elevation Angle Estimates Using Two Microphones**

**Kirsten A. Walker and W.C. Kirkpatrick Alberts, II**  
**Sensors and Electron Devices Directorate, ARL**

REPORT DOCUMENTATION PAGE			Form Approved OMB No. 0704-0188	
<p>Public reporting burden for this collection of information is estimated to average 1 hour per response, including the time for reviewing instructions, searching existing data sources, gathering and maintaining the data needed, and completing and reviewing the collection information. Send comments regarding this burden estimate or any other aspect of this collection of information, including suggestions for reducing the burden, to Department of Defense, Washington Headquarters Services, Directorate for Information Operations and Reports (0704-0188), 1215 Jefferson Davis Highway, Suite 1204, Arlington, VA 22202-4302. Respondents should be aware that notwithstanding any other provision of law, no person shall be subject to any penalty for failing to comply with a collection of information if it does not display a currently valid OMB control number.</p> <p><b>PLEASE DO NOT RETURN YOUR FORM TO THE ABOVE ADDRESS.</b></p>				
1. REPORT DATE (DD-MM-YYYY) June 2014		2. REPORT TYPE Final		3. DATES COVERED (From - To)
4. TITLE AND SUBTITLE Acoustic Source Elevation Angle Estimates Using Two Microphones		5a. CONTRACT NUMBER		
		5b. GRANT NUMBER		
		5c. PROGRAM ELEMENT NUMBER		
6. AUTHOR(S) Kirsten A. Walker and W.C. Kirkpatrick Alberts, II		5d. PROJECT NUMBER		
		5e. TASK NUMBER		
		5f. WORK UNIT NUMBER		
7. PERFORMING ORGANIZATION NAME(S) AND ADDRESS(ES) U.S. Army Research Laboratory ATTN: RDRL-SES-P 2800 Powder Mill Road Adelphi, MD 20783-1197		8. PERFORMING ORGANIZATION REPORT NUMBER ARL-TR-6976		
9. SPONSORING/MONITORING AGENCY NAME(S) AND ADDRESS(ES)		10. SPONSOR/MONITOR'S ACRONYM(S)		
		11. SPONSOR/MONITOR'S REPORT NUMBER(S)		
12. DISTRIBUTION/AVAILABILITY STATEMENT Approved for public release; distribution unlimited.				
13. SUPPLEMENTARY NOTES				
14. ABSTRACT Acoustic elevation angle estimates of airborne sources can be significantly degraded by interference between direct and ground-reflected signals. It has been shown, using a microphone vertically separated from a ground-based microphone, that elevation angle estimates of a passing aircraft could be improved by invoking the plane wave reflection coefficient and the geometry of the microphones. That approach is generalized here to include situations where the microphones are separated in two dimensions and where both microphones are elevated. Elevation angles are successfully estimated, under certain conditions, for a loudspeaker broadcasting band limited white noise.				
15. SUBJECT TERMS Acoustics, ground impedance, elevation estimation				
16. SECURITY CLASSIFICATION OF:			17. LIMITATION OF ABSTRACT  UU	18. NUMBER OF PAGES  24
A. Report Unclassified	b. ABSTRACT Unclassified	c. THIS PAGE Unclassified		
				19b. TELEPHONE NUMBER (Include area code) (301) 394-2121

---

## Contents

---

<b>by Kirsten A. Walker and W.C. Kirkpatrick Alberts, II</b>	<b>1</b>
<b>List of Figures</b>	<b>iv</b>
<b>List of Tables</b>	<b>iv</b>
<b>Acknowledgments</b>	<b>v</b>
<b>1. Introduction</b>	<b>1</b>
<b>2. Theory</b>	<b>1</b>
<b>3. Methods</b>	<b>4</b>
3.1 Procedures for Obtaining Base Ground Parameters .....	4
3.2 Transfer Function Measurement Procedures.....	6
<b>4. Results and Analysis</b>	<b>7</b>
<b>5. Concluding Remarks</b>	<b>11</b>
<b>6. References</b>	<b>12</b>
<b>Appendix. Transfer Functions</b>	<b>13</b>
<b>Distribution List</b>	<b>16</b>

---

## List of Figures

---

Figure 1. Microphone geometries used in generalizing the formulation of Williams et al. (a), Generalization 1 (b), Generalization 2 (c), and Generalization 3 (d). In sketches a and b, red represents the direct wave and green represents the ground reflected wave. Dashed arrows in c and d represent the images of the ground-reflected signals that reach each microphone. ....	2
Figure 2. ANSI standard setup, “geometry B,” on a grass field. ....	5
Figure 3. A diagram showing the placement of each configuration in relation to the noise source. Configurations shown are Williams (a), Generalization 1 (b), Generalization 2 (c), and Generalization 3 (d). ....	7
Figure 4. ANSI Geometries-A and -B plots with error bars at approximate third-octave frequencies. Measured transfer function in blue and fit transfer function in red. ....	8
Figure 5. Plots showing measured (blue) and fit (red) transfer functions for microphone configurations Williams (a), Generalization 1 (b), Generalization 2 (c), and Generalization 3 (d) at a 17.55° elevation angle. ....	9
Figure 6. Magnitude of the plane wave reflection coefficient calculated using parameters obtained by ANSI Geometry-A for each source height. ....	11
Figure A-1. Measured (blue) and fit (red) transfer functions for elevation angle of 4.06°, level 1. The Williams configuration is shown in (a), Generalization 1 in (b), Generalization 2 in (c), and Generalization 3 in (d). ....	13
Figure A-2. Measured and fit transfer functions for an elevation angle of 7.53°, level 2. Color and letter designations are the same as in figure A-1. ....	14
Figure A-3. Measured and fit transfer function for an elevation angle of 10.96°, level 3. Color and letter designations are the same as in figure A-1. ....	14
Figure A-4. Measured and fit transfer functions for an elevation angle of 14.31°, level 4. Color and letter designations are the same as in figure A-1. ....	15

---

## List of Tables

---

Table 1. Elevation angle estimates and the true angle for each configuration at each source level. ....	10
Table 2. Reflection coefficients for each configuration. ....	10
Table 3. Cumulative fit errors between measured and calculated transfer functions. ....	10

---

## Acknowledgments

---

We would like to thank Dr. Duong Tran-Luu for discussions regarding the derivations used in this work.

INTENTIONALLY LEFT BLANK.

---

## 1. Introduction

---

The U.S. Army uses acoustic arrays to track and locate various sources including ground and airborne vehicles, small arms, mortars, and rockets. The tracking and locating algorithms often used with these acoustic arrays perform well when estimating the azimuth of acoustic sources, but their performance decreases when estimating elevation angles (1, 2). Array performance can be reduced by environmental factors like wind, temperature, terrain, and acoustic impedance of the ground (2). A paper by Williams et al. (3) demonstrated that two vertically separated microphones, one in contact with the ground, could be used to significantly increase the accuracy of the estimated elevation angle of a passing aircraft. To accomplish the increase in elevation accuracy, the authors incorporated the ground impedance, using the plane-wave reflection coefficient, into the signal model used in the time delay of arrival calculations. In a recent article, Kruse and Taherzadeh demonstrate that a vertical array of eight microphones can be used to estimate the position of an elevated source by incorporating the spherical wave reflection coefficient into the source model of their beamformer (4). This report presents elevation angle estimates computed by a generalization of the formulation presented in Williams et al. (2).

The next section provides a description of the theoretical formulation used to determine elevation angle estimates. Section 3 describes experimental configurations used to measure ground parameter information and for verifying the theory developed in section 2. Experimental results and analysis are presented in section 4. Some concluding remarks are given in section 5.

---

## 2. Theory

---

Williams et al. described a simplified method for incorporating the plane-wave reflection coefficient into the signal model of an elevated moving source to improve the estimated elevation angle over traditional time delay of arrival estimates (2). They mention a signal at the ground,  $m_1(t) = Ds(t)$ , where  $s(t)$  is the direct signal reaching the microphone and  $D$  is a constant taking care of potential pressure doubling at the surface. At a microphone placed at a height  $h$  above the ground microphone, the signal is  $m_2(t) = s(t - \tau_1) + R(t)s(t - \tau_2)$ , where  $R(t)$  is the plane-wave reflection coefficient,  $\tau_1$  is the delay between the direct wave reaching the bottom microphone and the top microphone, and  $\tau_2$  is the delay between the ground-reflected wave at the top and bottom microphones (figure 1a). To obtain the transfer function between the two microphones, each time-domain signal is Fourier transformed and becomes

$$\begin{aligned}
M_1(f) &= DS(f) \\
M_2(f) &= S(f)e^{-i\omega\tau_1} + R(f)S(f)e^{-i\omega\tau_2}
\end{aligned} \tag{1}$$

The frequency domain formulation of the plane-wave reflection coefficient is  $R(f) = (1 - Z \cos \theta) / (1 + Z \cos \theta)$ , where  $Z$  is the normalized specific acoustic impedance of the ground and  $\theta$  is the incident angle of the source (measured relative to the surface normal). Using equation 1, the frequency-domain signal at the top microphone is divided by the signal at the bottom microphone to yield the transfer function

$$H_{M_1 M_2}(f) = \frac{M_2(f)}{M_1(f)} = \frac{e^{i\omega \frac{h}{c} \sin \theta} + R(f)e^{-i\omega \frac{h}{c} \sin \theta}}{D} \tag{2}$$

where it is noted that  $\tau_1 = -\tau_2 = \frac{h}{c} \sin \theta$  (see figure 1a) (2). Following Williams et al., the difference between the measured transfer function and equation 2 is minimized while constraining  $R$  to be between  $-1$  and  $1$  for all frequencies and  $\theta$  to be less than  $90^\circ$  (2). For the presentation here,  $D$  is fixed at 2. The minimization is accomplished using a grid search over the calculated transfer function.

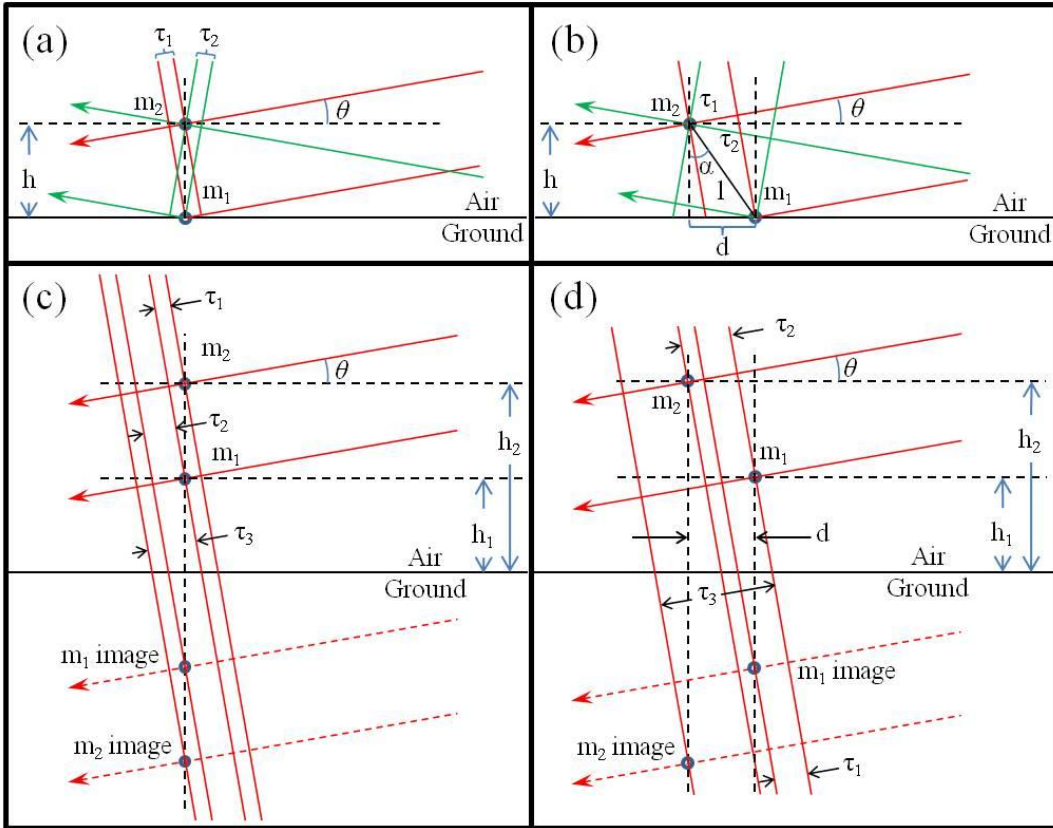


Figure. 1. Microphone geometries used in generalizing the formulation of Williams et al. (a), Generalization 1 (b), Generalization 2 (c), and Generalization 3 (d). In sketches a and b, red represents the direct wave and green represents the ground reflected wave. Dashed arrows in c and d represent the images of the ground-reflected signals that reach each microphone.

Because typical deployed acoustic arrays rarely have ground-based microphones or pairs of microphones separated only in the vertical, the formulation described by Williams et al. must be generalized to include pairs of elevated microphones separated horizontally as well as vertically. This is done in three steps: (1) generalize by translating the bottom microphone horizontally away from the elevated microphone, (2) generalize by elevating both microphones, and (3) generalize by translating the elevated bottom microphone horizontally away from the top microphone (figures 1b through 1c, respectively). The three steps in following discussions are referred to as Generalization 1, Generalization 2, and Generalization 3, respectively.

Generalizations 1 through 3 proceed similarly to the original formulation. However, for each generalization, it is noted that the delays between various arrivals (defined by the geometry of each generalization) change. As seen in figure 1b in the sketch of Generalization 1,  $\tau_1$  and  $\tau_2$  become

$$\begin{aligned}\tau_1 &= \frac{l}{c} \sin(\alpha - \theta) = \frac{\sqrt{h^2 + d^2}}{c} \sin \left[ \arctan \left( \frac{d}{h} \right) - \theta \right] \\ \tau_2 &= \frac{l}{c} \sin(\alpha + \theta) = \frac{\sqrt{h^2 + d^2}}{c} \sin \left[ \arctan \left( \frac{d}{h} \right) + \theta \right]\end{aligned}\quad (3)$$

Replacing  $\tau_1$  and  $\tau_2$  in equation 1 yields the transfer function for Generalization 1:

$$H_{M_1 M_2}(f) = \frac{e^{-i\omega \frac{\sqrt{h^2 + d^2}}{c} \sin \left[ \arctan \left( \frac{d}{h} \right) - \theta \right]} + R(f) e^{-i\omega \frac{\sqrt{h^2 + d^2}}{c} \sin \left[ \arctan \left( \frac{d}{h} \right) + \theta \right]}}{D}\quad (4)$$

Equation 4 is used to estimate the elevation angle and the reflection coefficient under the same constraints as the previous geometry.

For Generalization 2 (figure 1c), there is the added complication that the bottom microphone has a delayed ground reflected arrival, so the signals become (assuming time flow relative to the direct arrival at the bottom microphone)

$$\begin{aligned}m_1(t) &= s(t) + R(t)s(t - \tau_2) \\ m_2(t) &= s(t - \tau_1) + R(t)s(t - \tau_3).\end{aligned}\quad (5)$$

It is observed in figure 1c that there are now three delays that can be determined geometrically:

$$\begin{aligned}\tau_1 &= \frac{h_2 - h_1}{c} \sin(\theta) \\ \tau_2 &= -\frac{2h_1}{c} \sin(\theta). \\ \tau_3 &= \frac{h_1 - h_2}{c} \sin(\theta)\end{aligned}\quad (6)$$

Following the above procedures, the transfer function for Generalization 2 becomes

$$H_{M_1 M_2}(f) = \frac{e^{i\omega \frac{h_2-h_1}{c} \sin \theta} + R(f)e^{i\omega \frac{h_1-h_2}{c} \sin \theta}}{1 + R(f)e^{-i\omega \frac{2h_1}{c} \sin \theta}}. \quad (7)$$

To obtain the elevation angle and reflection coefficient using equation 7, the grid fit procedure is followed using the same constraints as in Williams et al.

For Generalization 3 (figure 1d), the bottom microphone is translated horizontally relative to the top microphone. The time delays relative to the direct wave at the bottom microphone become

$$\begin{aligned} \tau_1 &= -\frac{2h_1}{c} \sin(\theta) \\ \tau_2 &= -\frac{\sqrt{(h_2-h_1)^2 + d^2}}{c} \sin \left[ \arctan \left( \frac{d}{h_2-h_1} \right) - \theta \right]. \\ \tau_3 &= -\frac{\sqrt{(h_2+h_1)^2 + d^2}}{c} \sin \left[ \arctan \left( \frac{d}{h_2+h_1} \right) + \theta \right] \end{aligned} \quad (8)$$

Letting  $l = \sqrt{(h_2 - h_1)^2 + d^2}$ ,  $r = \sqrt{(h_2 + h_1)^2 + d^2}$ ,  $\alpha = \arctan \left( \frac{d}{h_2-h_1} \right)$ , and  $\beta = \arctan \left( \frac{d}{h_2+h_1} \right)$ , the transfer function becomes

$$H_{M_1 M_2}(f) = \frac{e^{-i\omega \frac{l}{c} \sin[\alpha-\theta]} + R(f)e^{-i\omega \frac{r}{c} \sin[\beta+\theta]}}{1 + R(f)e^{-i\omega \frac{2h_1}{c} \sin \theta}}. \quad (9)$$

As with the previous generalizations, the elevation angle and reflection coefficient are determined by a grid fit of equation 9 to the measured transfer function.

### 3. Methods

#### 3.1 Procedures for Obtaining Base Ground Parameters

The American National Standards Institute (ANSI) standard procedure was followed to deduce a baseline parameter set (figure 2) (3). These ground impedance parameter estimates were made using two Brüel and Kjær (B&K) type 4192 ½-in pressure-field microphones calibrated using a B&K Acoustic Variable Calibrator, type 4226. The source used for the ANSI procedures was a JBL model 2446H pressure driver coupled to a 1-m-long pipe with a 3.175 cm inner diameter. This source can be approximated as a point source to a frequency of approximately 2.7 kHz (3). An Agilent Technologies 35670A dynamic signal analyzer was used to generate a 250 Hz to 2.5 kHz swept sine signal and to record the magnitude response of each microphone. Wind speeds and directions were monitored with an Airmar LB150 ultrasonic anemometer at a height

of approximately 1.2 m, located roughly 25 m from the test area. The average wind speed throughout the day was 1.7 m/s with a standard deviation of 0.58 m/s.



Figure 2. ANSI standard setup, “geometry B,” on a grass field.

The ANSI standard prescribes the use of two geometries, A and B, to measure level differences over ground surfaces. Geometry-A consisted of two vertically spaced microphones at heights of 46.0 and 23.0 cm. The source was at a height of 32.5 cm and 1.75 m away from the microphones. Geometry-B had a source-microphone separation of 1 m with a source height of 20 cm and microphone heights of 20 and 5 cm (3).

Following the ANSI procedures to deduce ground parameter information necessitates fitting a calculated level difference to the difference in sound pressure level between the two measurement microphones. The level difference is calculated after assuming harmonic time dependence and noting that the pressure at each microphone is given by

$$p(f) = \frac{1}{R_d} \exp[ikR_d] + Q(f, \beta) \frac{1}{R_r} \exp[ikR_r] \quad (10)$$

In equation 10,  $R_d$  is the direct path length from the source to the microphone,  $R_r$  is the reflected path length,  $f$  is the frequency,  $k$  is the wave number, and  $Q$  is the spherical wave reflection coefficient (5) that depends upon frequency and the admittance,  $\beta$ , of the ground. The admittance is the inverse of the specific acoustic impedance of the ground. For the presentation here, the impedance was calculated with

$$Z = \frac{1+i}{\sqrt{\pi\gamma\rho_0}} \sqrt{\frac{\sigma_e}{f}} + \frac{ic_0\alpha_e}{8\pi\gamma f}, \quad (11)$$

where  $\gamma$  is the ratio of specific heats in air,  $\rho_0$  is the density of air,  $c_0$  is the speed of sound,  $\sigma_e$  is the effective flow resistivity of the ground, and  $\alpha_e$  is the rate of change of porosity with depth. Fit parameters are the flow resistivity and the rate of change of porosity. A Levenberg-Marquardt scheme was used to determine  $\sigma_e$  and  $\alpha_e$  by fitting calculated level differences to the measured level differences (6, 7).

### 3.2 Transfer Function Measurement Procedures

To investigate the validity of the transfer functions derived in section 2, the following procedures were used. A JBL EON15G2 speaker was used as the noise source and was placed on a tower at heights of approximately 1.83, 3.66, 5.49, 7.32, and 9.14 m. These heights are referred to as level 1, level 2, level 3, level 4, and level 5, respectively. The Agilent 35670A was used to generate band-limited random noise from 50–1650 Hz and to record average spectra (30 averages) from two ½-in B&K 4192 microphones. The grass at the test area was approximately 7–10 cm in length (see figure 2). The ground was saturated with water; pools of standing water were adjacent to the test site.

Figure 3 shows sketches of the experimental configurations used during the test. The two microphones, upper and lower, with open-cell foam windscreens, were placed approximately 30 m from the tower. The microphones were placed in four configurations: Williams, Generalization 1, Generalization 2, and Generalization 3. The Williams configuration had two vertically spaced microphones; the upper microphone at a height of 25 cm and the lower microphone placed on the ground. Generalization 1 had the upper microphone 25 cm above the ground and the lower microphone on the ground but translated 25 cm toward the sound source. Generalization 2 had the microphones vertically aligned with the upper microphone at a height of 50 cm and the lower microphone at a height of 25 cm. In the last configuration, Generalization 3, the upper microphone was at a height of 50 cm and the lower microphone was at a height of 25 cm and translated 25 cm toward the source. The test was repeated at each source height with the microphones in each of the four configurations, which yielded a total of 20 elevation angle estimates.

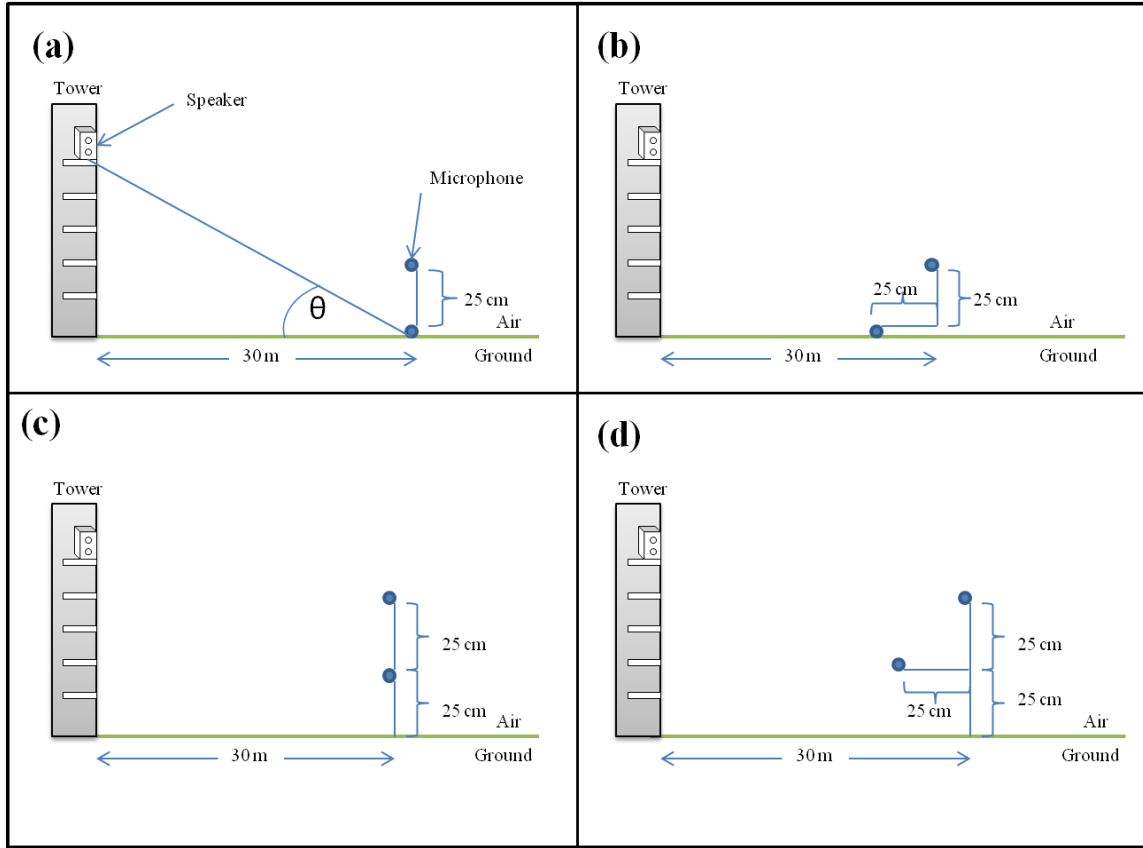


Figure 3. A diagram showing the placement of each configuration in relation to the noise source. Configurations shown are Williams (a), Generalization 1 (b), Generalization 2 (c), and Generalization 3 (d).

## 4. Results and Analysis

Figures 4a and b show the measured and the fit level differences for the ANSI Geometries-A and -B, respectively. In each plot, error bars show  $\pm$  one standard deviation at approximate third-octave frequencies. The insets in each plot show  $\sigma_e$ ,  $\alpha_e$ , and the cumulative error between the fit and the measurement for Geometry-A and -B. The parameter values obtained using the ANSI methods are consistent with previous measurements at the test range (6, 8) and are indicative of grassland (5).

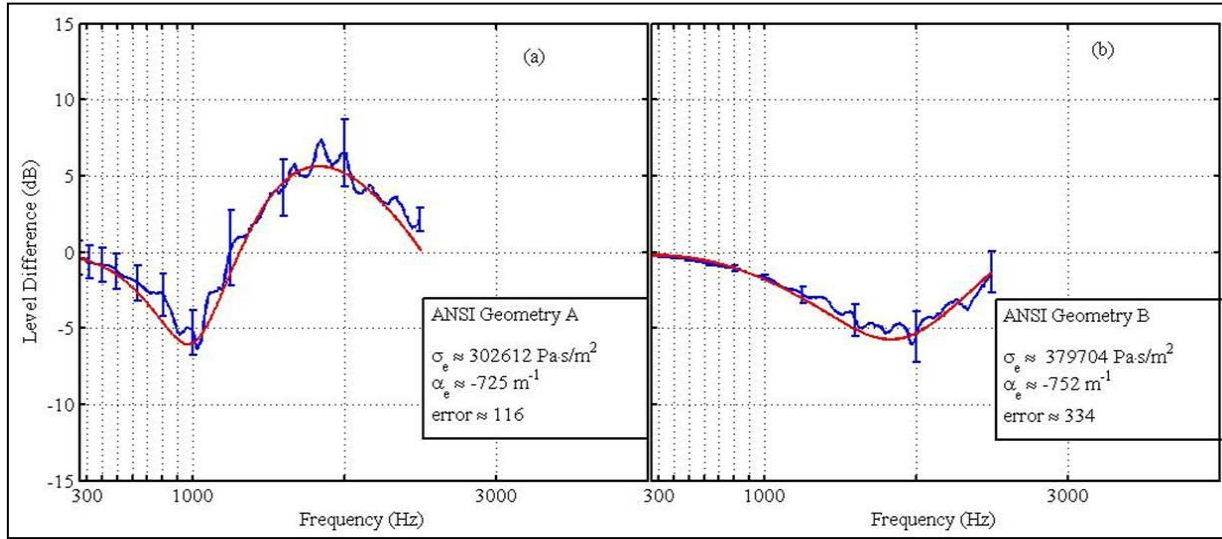


Figure 4. ANSI Geometries-A and -B plots with error bars at approximate third-octave frequencies. Measured transfer function in blue and fit transfer function in red.

Figure 5 shows plots from each of the four microphone configurations at an elevation angle of  $17.55^\circ$  (level 5); the measured transfer function is in blue and the fit transfer function is in red. In each inset the estimated angle, reflection coefficient and the error are shown. Another inset in each plot shows the microphone configuration with an arrow pointing in the direction of the source. The calculated transfer functions tend to follow the broad features in the measured transfer functions. The minimum at approximately 1 kHz in figures 5a and b appears to be skewed from the measured minimum, which may be due to the structure of the measured curve.

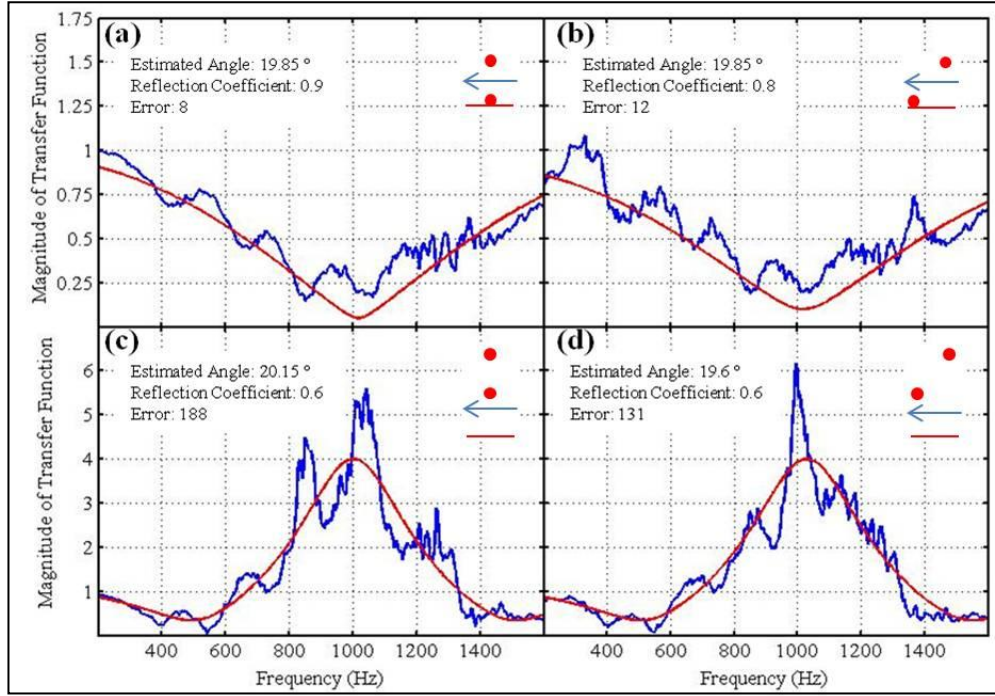


Figure 5. Plots showing measured (blue) and fit (red) transfer functions for microphone configurations Williams (a), Generalization 1 (b), Generalization 2 (c), and Generalization 3 (d) at a  $17.55^\circ$  elevation angle.

Tables 1 through 3 show the elevation angle estimates, reflection coefficients, and the cumulative fit errors, respectively, for each of the microphone configurations and for each source height. In table 1, angles estimated using Generalization 2 and 3 show significant errors at low source angles. However, at higher angles the estimates become comparable to those obtained from the Williams and Generalization 1 configurations. Williams and Generalization 1, which each have a ground microphone, tend to yield better angle estimates for all five angles. The reflection coefficients in table 2 are considered effective, because they were taken to be constant for all frequencies (see section 2). For Williams and Generalization 1 the effective reflection coefficients remain relatively constant for all angles, while the effective reflection coefficients obtained using Generalizations 2 and 3 tend to increase with increasing elevation angle. The cumulative fit errors (table 3) tend to increase with the source angle and the complexity of the microphone geometry.

Table 1. Elevation angle estimates and the true angle for each configuration at each source level.

<b>Geometry \ Level</b>	<b>1</b>	<b>2</b>	<b>3</b>	<b>4</b>	<b>5</b>
<b>True Angle</b>	<b>4.06°</b>	<b>7.53°</b>	<b>10.96°</b>	<b>14.31°</b>	<b>17.55°</b>
<b>Williams</b>	5.4°	7.3°	9.35°	18.85°	19.85°
<b>Generalization 1</b>	4.25°	8.05°	9°	18°	19.85°
<b>Generalization 2</b>	12.35°	13.2°	14.8°	17.7°	20.15°
<b>Generalization 3</b>	11.75°	12.7°	15.2°	17.1°	19.6°

Table 2. Reflection coefficients for each configuration.

<b>Geometry \ Level</b>	<b>1</b>	<b>2</b>	<b>3</b>	<b>4</b>	<b>5</b>
<b>Williams</b>	0.85	0.80	0.75	1.0	0.90
<b>Generalization 1</b>	0.85	0.80	0.80	0.80	0.80
<b>Generalization 2</b>	0.30	0.30	0.40	0.50	0.60
<b>Generalization 3</b>	0.35	0.35	0.40	0.50	0.60

Table 3. Cumulative fit errors between measured and calculated transfer functions.

<b>Geometry \ Level</b>	<b>1</b>	<b>2</b>	<b>3</b>	<b>4</b>	<b>5</b>
<b>Williams</b>	8.1	10.2	11.7	15.6	8.6
<b>Generalization 1</b>	9.3	11.2	10.7	18.2	12.1
<b>Generalization 2</b>	12.2	20.1	42.6	149.0	188.4
<b>Generalization 3</b>	11.1	16.2	39.2	66.1	131.1

Figure 6 shows the magnitude of the plane-wave reflection coefficient for each source height used here. The ground impedance was calculated using the base ground impedance parameters obtained from the procedures in section 3.1 in the two-parameter ground impedance model used in the ANSI standard, equation 11 (3). The curves in figure 6 show that, over the frequency range of interest, the plane-wave reflection coefficient varies significantly. The implication is that the effective coefficient obtained by holding R constant over all frequencies is overly simplified and, thus, tends to add error to the estimated elevation angle, which reinforces observations made in references 1 and 2. This error is apparent in the estimated angles shown in table 1; at angles

where the estimates are closest to the true angles, level 5, the reflection coefficient in figure 6 has the least overall variation.

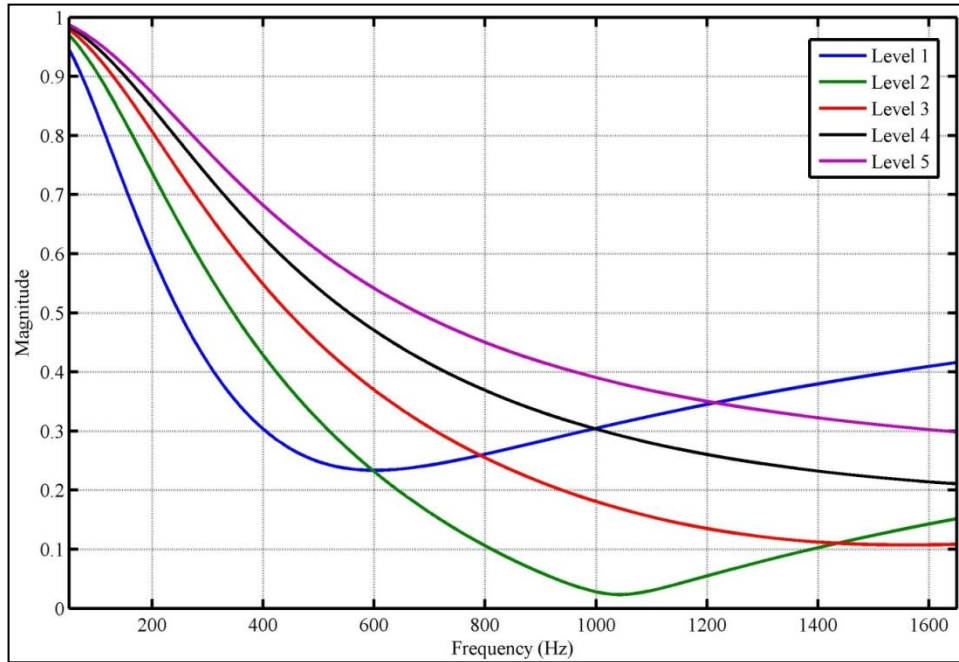


Figure 6. Magnitude of the plane wave reflection coefficient calculated using parameters obtained by ANSI Geometry-A for each source height.

The trends shown between the various angles and geometries imply that the assumptions used in deriving the transfer functions for increasingly complex microphone geometries break down once both microphones are elevated. Specifically, the assumption of a real reflection coefficient constant in frequency is over simplified. Further, at the source distance used in these experiments the plane wave reflection coefficient may not sufficiently capture the behavior of the reflected acoustic wave. For three-dimensional (3-D) arrays with ground-based microphones, the results reported here show that this type of processing will yield acceptable elevation angles, which is consistent with the results reported by Williams et al. (2).

## 5. Concluding Remarks

Acoustic transfer functions measured over grass at a U.S. Army test facility have demonstrated that the elevation angle of a nearby acoustic source can be successfully estimated using microphones separated in two dimensions. However, the elevation angles estimated using raised microphones become more correct as the source angle increases, implying that the assumptions used to calculate the transfer function are overly simplified.

---

## 6. References

---

1. Goldman, G. *Computationally Efficient Algorithms for Estimating the Angle of Arrival of Helicopters Using Acoustic Arrays*; ARL-TR-4998; U.S. Army Research Laboratory: Adelphi, MD, 2009.
2. Williams, J.; Williams, C.; Frazier, W. Enhancing Real-Time 3D Tracking of Acoustic Targets Using Elevated Microphones and Environmental Parameter Effects *Proc. SPIE* **2003**, 5090, 77–87.
3. S1.18-2010, *Method for Determining the Acoustic Impedance of Ground Surfaces*, American National Standard Institute, 2010.
4. Kruse, R.; Taherzadeh, S. The Influence of Environmental Conditions on Estimation of Source Distance and Height Using a Single Vertical Array. *APAC* **2012**, 73, 198–208.
5. Attenborough, K.; Bashir, I.; Taherzadeh, S. Outdoor Ground Impedance Models. *J. Acoust. Soc. Am.* **2011**, 129 (5), 2806–2819.
6. Alberts, II, W.C.K.; Sanchez, K. J. Deduction of the Acoustic Impedance of The Ground Via a Simulated Three-Dimensional Microphone Array. *J. Acoust. Soc. Am.* **2013**, 134 (5), EL471–EL476.
7. Press, W. H.; Flannery, B. P.; Teukolsky, S. A.; Vetterling, W. T. *Numerical Recipes in C: The Art of Scientific Computing*, Cambridge University Press, New York, 1988.
8. Alberts, II, W.C.K.; Coleman, M. A.; Noble, J. M. *Characterization of Acoustic Ground Impedance at Blossom Point Research Facility*; ARL-TR-5352; U.S. Army Research Laboratory: Adelphi, MD, 2010.

---

## Appendix. Transfer Functions

---

Shown in this appendix are plots (figures A-1 through A-4) of the remaining measured and fit transfer functions for each of the geometries not shown in section 4. In all plots, the Williams configuration is shown in (a), Generalization 1 in (b), Generalization 2 in (c), and Generalization 3 in (d). For all plots the measured transfer function is in blue and the fit transfer function is in red.

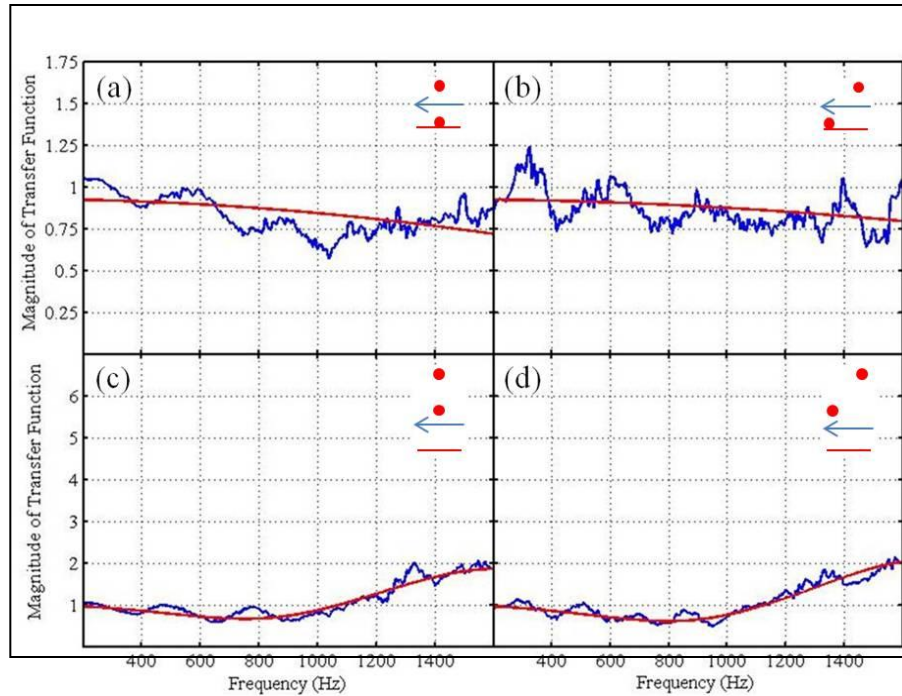


Figure A-1. Measured (blue) and fit (red) transfer functions for elevation angle of  $4.06^\circ$ , level 1. The Williams configuration is shown in (a), Generalization 1 in (b), Generalization 2 in (c), and Generalization 3 in (d).

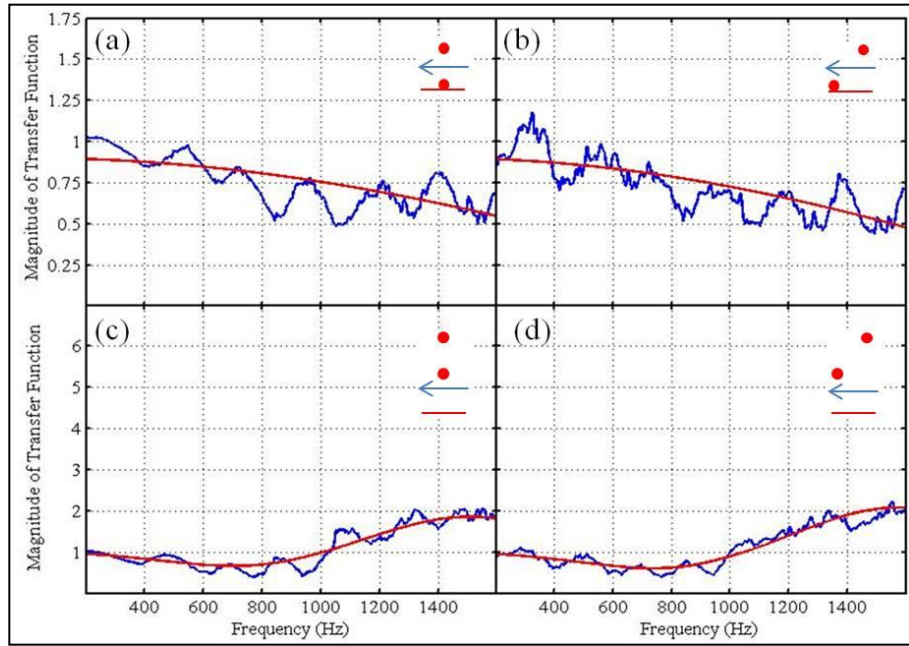


Figure A-2. Measured and fit transfer functions for an elevation angle of  $7.53^\circ$ , level 2. Color and letter designations are the same as in figure A-1.

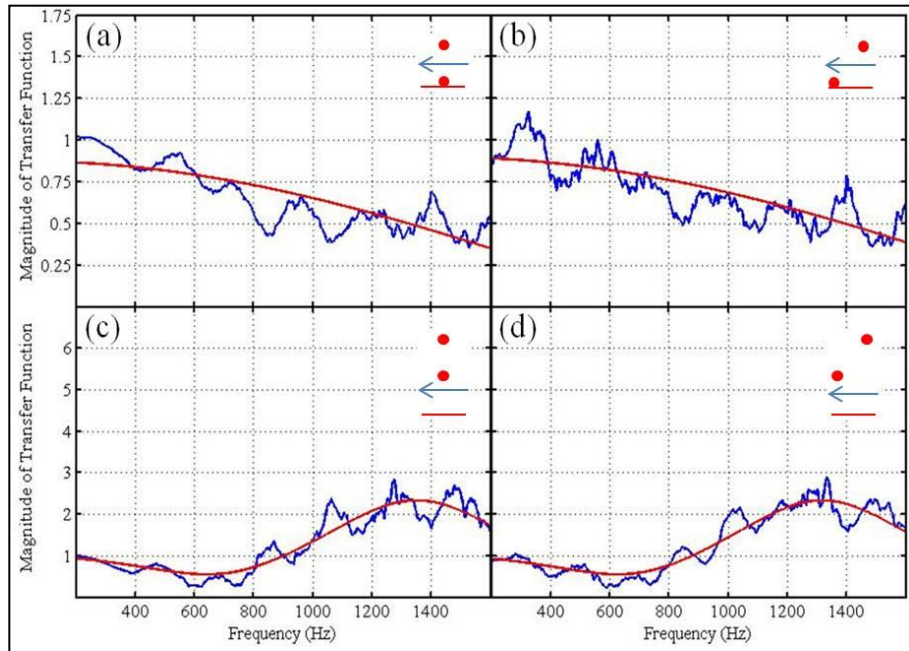


Figure A-3. Measured and fit transfer function for an elevation angle of  $10.96^\circ$ , level 3. Color and letter designations are the same as in figure A-1.

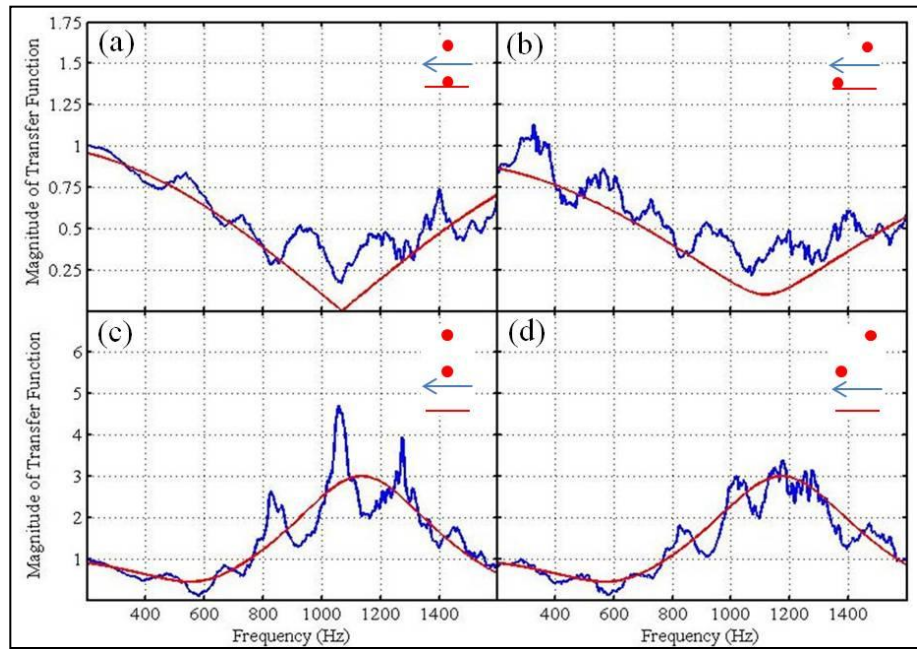


Figure A-4. Measured and fit transfer functions for an elevation angle of  $14.31^\circ$ , level 4.  
Color and letter designations are the same as in figure A-1.

1 DEFENSE TECHNICAL  
(PDF) INFORMATION CTR  
DTIC OCA

2 DIRECTOR  
(PDF) US ARMY RESEARCH LAB  
RDRL CIO LL  
IMAL HRA MAIL & RECORDS MGMT

1 GOVT PRINTG OFC  
(PDF) A MALHOTRA

2 DIRECTOR  
(PDF) US ARMY RESEARCH LAB  
RDRL SES P  
KIRSTEN A. WALKER  
W.C. KIRKPATRICK ALBERTS II